scientific reports

Check for updates

OPEN

miR-27a-3p promotes inflammatory response in infectious endophthalmitis via targeting TSC1

Yanting Chen✉, Shanxiang Li & Hong He

Infectious endophthalmitis (IE) poses a significant threat to vision. This study aimed to explore the impact of microRNA (miR)-27a-3p on inflammation in IE. A rat model was developed through intravitreal injection of lipopolysaccharide. Clinical and demographic data were collected for 54 participants: 31 diagnosed with IE and 23 non-infectious patients with idiopathic macular holes. Expression levels of miR-27a-3p and inflammatory genes were quantified via reverse transcription quantitative polymerase chain reaction. Concentrations of inflammatory cytokines in human vitreous samples were measured using enzyme-linked immunosorbent assay. In vitro studies were conducted to explore the target gene of miR-27a-3p. The final animal experiments further verified the role of miR-27a-3p and tuberous sclerosis complex (TSC)1 in inflammatory responses. Results showed that miR-27a-3p was elevated in LPS-treated rats and IE patients. Thirty-one IE patients were divided into the High (n = 15) and Low (n = 16) groups according to the expression of miR-27a-3p. No significant differences were observed in baseline clinical and demographic characteristics between the control and IE patient groups. Pro-inflammatory cytokine mRNA levels and concentrations were notably increased in both LPS-treated rats and the High group of patients. Besides, results showed that TSC1 is a target gene of miR-27a-3p. Moreover, TSC1 inhibition promoted inflammation in rat vitreous samples. In summary, our findings suggested that miR-27a-3p exacerbated inflammatory responses in IE though targeting TSC1, offering novel insights for potential therapeutic strategies targeting miR-27a-3p in the clinical management of IE.

Keywords Infectious endophthalmitis, miR-27a-3p, TSC1, Inflammatory response, Cytokines

Endophthalmitis, a severe ocular condition, is bifurcated into infectious endophthalmitis (IE) and non-infectious endophthalmitis. IE arises from microbial invasion into ocular tissues, triggering an inflammatory cascade. Despite its relatively low prevalence, IE represents a significant threat to visual acuity, often precipitating symptoms such as vision loss, ocular discomfort, and in extreme cases, necessitating enucleation[1]. The vitreous humor, occupying the largest volume within the eye, resides posteriorly between the lens and retina. Characterized by its clear, gelatinous consistency primarily composed of water[2], it plays a pivotal role in maintaining the eye's structural integrity. Key clinical manifestations of IE encompass conjunctival injection, sudden vision decline, and vitreous opacification. While intravitreal antibiotic administration constitutes the cornerstone of IE therapy, persistent inflammation and recurrence pose ongoing challenges[3,4]. Consequently, elucidating the underlying pathophysiological mechanisms of IE and identifying innovative therapeutic targets becomes imperative.

Cytokines, as key intercellular signaling molecules, function as chemical messengers and chemoattractants, orchestrating the initiation, maintenance, and resolution phases of immune responses[5]. Secreted by leukocytes, including lymphocytes and macrophages, as well as ocular resident cells, they underpin critical biological processes such as antigen recognition, leukocyte recruitment, pathogen clearance, and tissue repair[5]. This dual role encompasses both pro-inflammatory and anti-inflammatory cytokines, which are integral to immune regulation[6]. Pro-inflammatory cytokines serve as the vanguard in infectious and non-infectious inflammatory conditions, driving and perpetuating the inflammatory cascade. Conversely, anti-inflammatory cytokines, acting as a counterbalance, exert regulatory functions over their pro-inflammatory counterparts, fine-tuning the immune response to prevent tissue damage[6]. In the context of IE, cytokine profiles are markedly altered. Studies

Hainan Eye Hospital and Key Laboratory of Ophthalmology, Zhongshan Ophthalmic Center, Sun Yat-Sen University, No.19 Xiuhua Road, Xiuying District, Haikou 570311, Hainan, China. ✉email: bery1455@126.com

employing animal models of IE have consistently shown elevated levels of pro-inflammatory cytokines, namely interleukin (IL)-1β, IL-6, IL-8, interferon (IFN)-γ, and tumor necrosis factor (TNF)-α[5]. For example, in a murine model infected with Aspergillus fumigatus, there is a pronounced upregulation of TNF-α, IL-1β, and IL-6[7]. This pattern is mirrored in other ocular disorders, such as diabetic retinopathy[8] and glaucoma[9], underscoring the multifaceted roles cytokines play in ocular health and disease.

MicroRNAs (miRs), pivotal post-transcriptional regulators, function by binding to the 3′ untranslated region (3'UTR) of target messenger RNAs (mRNAs), thereby modulating gene expression[10]. Among them, miR-27a-3p, situated on chromosome 19 (19p13.1) and comprising 21 nucleotides in length[11], has garnered attention for its involvement in diverse pathologies[10,12–14]. Notably, earlier research has documented elevated levels of miR-27a-3p in aged retinas relative to younger counterparts[15], hinting at its potential role in age-related ocular changes. Furthermore, aberrant expression of miR-27a-3p has been linked to diabetic retinopathy, contributing to the impairment of human retinal endothelial cells[16]. Emerging evidence suggests that this miRNA amplifies disease progression by instigating inflammatory pathways[17,18]. Despite these insights, the specific contribution of miR-27a-3p to IE remains unexplored, warranting further investigation.

This study aims to investigate the role of miR-27a-3p in IE in tropical regions of China.

Methods and materials

Establishment of rat model and sample collection

Animal experiment protocols in this study were approved by the Animal Ethics Committee of Hainan Eye Hospital and Key Laboratory of Ophthalmology, Zhongshan Ophthalmic Center, Sun Yat-sen University. All methods were carried out in accordance with relevant guidelines and regulations. All methods are reported in accordance with ARRIVE guidelines for the reporting of animal experiments.

Experiment I

Thirty male Sprague–Dawley rats (180–200 g), sourced from Charles River (Beijing, China), were maintained under specific pathogen-free conditions at a controlled temperature of 25 °C with a regulated 12-h light/dark cycle. These animals were randomly allocated to two groups: a control group and a lipopolysaccharide (LPS; Sigma Cambridge, MA, USA) group, each consisting of 15 rats. LPS (Sigma) was dissolved in sterile saline (Sigma) to achieve a concentration of 0.2 g/L. Prior to the experimental procedure, each rat received 1 mg/kg ketamine (Sigma) as a baseline anesthetic. Under microscopic guidance, rats in the LPS group were administered a 5 µL intravitreal injection of the LPS solution directly into the vitreous cavity, positioned 1 mm posterior to the corneoscleral limbus, utilizing a 30-gauge needle and a 10 µL microsyringe. In contrast, the control group underwent an identical procedure, substituting the LPS solution with 5 µL of sterile saline. Notably, all intravitreal injections were performed exclusively in the right eye of each rat.

At predetermined intervals post-LPS injection—0 h, 24 h, 3 d, and 7 d, three rats were sequentially selected from each group. Euthanasia was induced via an intraperitoneal injection of 3% pentobarbital sodium (Sigma). Immediately thereafter, the eyeballs were excised, and the retina tissues were meticulously isolated and flash-frozen in liquid nitrogen for preservation. Simultaneously, the remaining eyeballs were longitudinally sectioned on an ice-cooled platform. Following the removal of the crystalline lens, vitreous samples were harvested. To maintain sample integrity, 2.5 mL of ice-cold saline per gram of tissue was added to the vitreous samples. Using an ultrasonic homogenizer, the samples were processed under cryogenic conditions to create a vitreous homogenate. Subsequently, the homogenate underwent centrifugation at $16{,}000 \times g$ for 10 min at 4 °C. The resultant supernatant was carefully collected and stored at − 80 °C for subsequent analyses.

Experiment II

Twenty-four rats were randomly divided into four groups: control, LPS, LPS + AntagomiR-27a-3p + LV-sh-NC, and LPS + AntagomiR-27a-3p + LV-sh-tuberous sclerosis complex (TSC)1, with six rats in each group. The LPS group rats were treated with LPS for 24 h. Each rat in the LV-sh-NC or LV-sh-TSC1 groups was intravenously administered 5×10^7 TU LV-sh-NC or LV-sh-TSC1 in 200 µL PBS once a week continuously for four weeks. To inhibit the expression of miR-27a-3p in vivo, the rats were then injected with the miR-27a-3p antagomiR (200 nM; RiboBio Biotech Co., Ltd., Guangzhou, China) through the tail vein and administered every other day for a total of seven times. Finally, retinal and vitreous tissues of all rats were collected and stored according to the methods in experiment I.

Hematoxylin–eosin (H&E) staining

Rat retina tissues were fixed in 10% formaldehyde solution (Thermo Fisher Scientific, Carlsbad, CA, USA) for 48 h, followed by a thorough washing under running water for 24 h. Subsequently, tissues underwent routine paraffin embedding using an automated embedding station (Leica Microsystems Trading LTD., Shanghai, China). The embedded tissues were then sectioned into slices of 5 µm thickness. To prepare the sections for histological analysis, they were placed in an incubator maintained at 60 °C (Bowen Instrument Co., Ltd., Shanghai, China) for 1 h. Following incubation, sections were deparaffinized with xylene (Thermo Fisher Scientific) and rehydrated through a graded series of ethanol washes (Thermo Fisher), concluding with a water rinse. Hematoxylin staining (Beyotime Biotechnology, Shanghai, China) was applied for 10 min, after which sections were rinsed under running water to remove excess stain. Differentiation was achieved with a brief immersion in 5% acetic acid (Thermo Fisher) for 1 min, before proceeding to eosin staining (Beyotime Biotechnology) for 3 min. Upon completion of staining, sections were dehydrated, cleared in xylene, and mounted using neutral balsam (Solarbio Science & Technology Co. Ltd., Beijing, China) once dried. Digital images of the stained sections were acquired using an optical microscope (Pulnix, Sunnyvale, CA, USA) equipped with a digital camera for high-resolution imaging.

Preparation of miR samples and microRNA sequencing (miR-seq)

Total RNA was isolated from rat retina tissues using Trizol Reagent (Vazyme Biotechnology Co., LTD., Nanjing, China), and the concentration and quality were measured using a NanoDrop spectrophotometer (Thermo Fisher). NEBNext Multiplex Small RNA Library Prep Set for Illumina (New England Biolabs Inc., Ipswich, MA, USA) was used for constructing small RNA libraries based on the manufacturer's instructions. Briefly, 1 μg total miRs was ligated to 3′ and 5′ adapters using Ligation Enzyme Mix. Ligated RNA products were reverse transcribed using Superscript II reverse transcriptase and amplified by polymerase chain reaction. Small RNA libraries were quality controlled and quantified using the Agilent High Sensitivity DNA Assay on the Bioanalyzer 2100 System. The small RNA library was then sequenced on NovaSeq 6000 platform (Illumina, San Diego, CA, USA) by Personal Biotechnology Co. Ltd. (Shanghai, China).

miR sequencing data analysis

Differentially expressed miRs were identified using DESeq (v1.18.0, https://www.huber.embl.de/users/anders/DESeq/). R language was used to analyze the data, and the differentially expressed miRs were defined as $p < 0.05$ and $|\log2(\text{fold change})| > 1$. Pheatmap software package of R was used to perform bidirectional cluster analysis on all miRs. The distance was calculated by the Euclidean method, and miRs were clustered using the hierarchical clustering longest distance method (Complete Linkage). Heatmap was made by the HemI 1.0 software (http://hemi.biocuckoo.org/index.php).

Human study design and sample collection

This study was approved by Hainan Eye Hospital and Key Laboratory of Ophthalmology, Zhongshan Ophthalmic Center, Sun Yat-sen University. The study included 31 patients diagnosed with IE and 23 non-infectious patients with idiopathic macular holes. Patients were excluded if the vitreous sample was inadequate after routine microbiology workup. Basic information of all patients was collected and shown in Table 1. All patients underwent complete ophthalmological examinations, including B-scans, slit-lamp biomicroscopy, and visual acuity (VA) measurements. The best-corrected visual acuity measurements were converted to the logarithm of the minimum angle of resolution (logMAR)[19] for comparative analysis. The initial VA was recorded on the same day of the

Characteristic	Controls (n = 23)	Infectious endophthalmitis (n = 31) miR-27a-3p		*p*-value
		High (n = 15)	Low (n = 16)	
Age (yr), median ± SD	41.17 ± 15.44	55.73 ± 18.66	47.88 ± 16.87	0.228
Gender (male:female), n	13:10	7:8	10:6	0.376[a]
Diagnosis, n				–
Postoperative (cataract surgery)	–	8	7	
Traumatic	–	3	5	
Endogenous	–	4	4	
Macular hole/macular edema	20	–	–	
Rhegmatogenous retinal detachment	3	–	–	
Initial visual acuity (logMar)				–
0.6–2	10	8	4	
2.6	8	3	4	
3.2	5	4	8	
Final visual acuity (logMar)				–
0.4–1.3	7	5	3	
2–2.9	7	6	5	
3–3.2	9	4	8	
Evisceration, n	–	–	–	
Inflammation/polymorphs (vitreous), n				–
0–3	–	3	5	
0–5	–	3	6	
0–10/0–plenty	–	9	5	
Surgical interventions, n				–
< 2	21	4	9	
≥ 2	2	11	5	
Pathogenic microorganisms				–
Gram positive	–	9	12	
Gram negative	–	1	0	
Fungal	–	5	4	

Table 1. Clinical characteristics of the study population. [a]Pearson's $\chi 2$ test.

endophthalmitis diagnosis and the final VA after six months of follow-up. The vitreous samples were aseptically collected from all 54 patients during vitrectomy and transferred into a presterilized microcentrifuge tube, and stored at -80 °C for further analysis.

Reverse transcription-quantitative polymerase chain reaction (RT-qPCR)

Human vitreous samples miR was obtained by the miRNeasy Mini Kit (Qiagen, Venlo, Netherlands) according to the manufacturer's instructions. Total RNA from rat vitreous samples was extracted by TriZOL. The quality and concentration of miR and RNA were detected using a NanoDrop spectrophotometer. miR 1st Strand cDNA Synthesis Kit and HiScript III 1st Strand cDNA Synthesis Kit (Vazyme) were used for reverse transcription. Real time PCR was carried out using the miScript SYBR Green PCR kit (Qiagen) and Taq Pro Universal SYBR qPCR Master Mix kit (Vazyme) according to the provided conditions. The used primers were obtained from Genescript Biotech Co., LTD., (Nanjing, China) and listed in Table 2. RNU6B and GAPDH were used as the internal control. The genes expression were calculated by the $2^{-\Delta\Delta CT}$ method.

Enzyme-linked immunosorbent assay (ELISA)

The expression of IL-1α, IL-6, IL-8, IL-10, TNF-α, IFN-γ and granulocyte–macrophage colony-stimulating factor (GM-CSF) in human vitreous samples were detected by specific ELISA kits (KangChen Biotechnology Co. Ltd., Shanghai, China) according to the instructions. The antibody was diluted with carbonate buffer (0.05 M, pH 9.6) to a protein content of 1–10 μg/ml. Then, 0.1 ml of diluted antibody was added to polystyrene plate at 4℃ overnight. The next day, the solution was discarded and the well was washed by washing buffer 3 times, for 3 min each time. Then, 0.1 mL of prepared vitreous supernatant was incubated at 37 °C for 1 h, followed by incubated with 0.1 mL of freshly diluted enzyme labeled antibody at 37 °C for 30 min. Subsequently, 0.1 mL of tetramethyl benzidine substrate solution was added to each well to incubate at 37 °C for 30 min. A total of 0.05 mL of sulfuric acid (2 M) was added to stop the reaction. The absorbance of each well was measured at 450 nm on the microplate reader (Thermo Fisher).

Bioinformatic analysis

The Targetscan (https://www.targetscan.org/vert_80/), starbase (https://rnasysu.com/encori/panCancer.php), and MicroRNA Target Prediction (miRDB; https://mirdb.org/) databases were used to predict the suspicious

Name	Forward (5′-3′)	Reverse (5′-3′)
miR-27a-3p	CCGCTCGAGACTGGCTGCTAGGAAGGTG	GCGAATTCTTGCTGTAGCCTCCTTGTC
RNU6B	GCGAATTCTTGCTGTAGCCTCCTTGTC	AACGCTTCACGAATTTGCGT
TNF-α	GTGAGGAGGACGAACATC	GAGCCAGAAGAGGTTGAG
IL-1β	CCGTGGACCTTCCAGGATGA	GGGAACGTCACACACCAGCA
TSC1	CAACAAGCAAATGTCGGGGAG	CATAGGGCCACGGTCAGAA
ID4	TCCCGCCCAACAAGAAAGTC	CCAGGATGTAGTCGATAACGTG
PAX9	GGAGGAGTGTTCGTGAACGG	CGGCTGATGTCACACGGTC
PLEKHH1	GGTGACACTCAAGTTGGCAAA	TCTGAATAGCTTCTAGCGCATCT
NRP2	GCTGGCTATATCACCTCTCCC	TCTCGATTTCAAAGTGAGGGTTG
TMCC1	AAGTCTGGTCAGGAGATGACAG	TACTTCCAACCGTTCGATCCG
RUNX1	CTGCCCATCGCTTTCAAGGT	GCCGAGTAGTTTTCATCATTGCC
CDR2	ATGCTGGCGGAAAACCTGG	CCACTTGCTTCGTCAGATACTC
B4GALT3	CGAGATCAGGGACCGACATTT	GATCGTTCTGGACAGTAGGGC
SYNRG	TCATGCAGCCTAATATGCAAGG	GCATTGGTCCCATTGGTATTCC
HIPK2	CCCGTGTACGAAGGTATGGC	AGTTGGAACTCGGCTCTATTTTC
SEMA7A	TTCAGCCCGGACGAGAACT	GAACCGAGGGATCTTCCCAT
RELN	CAACCCCACCTACTACGTTCC	TCACCAGCAAGCCGTCAAAAA
PDK4	GGAGCATTTCTCGCGCTACA	ACAGGCAATTCTTGTCGCAAA
ST6GALNAC3	TGCTGGTTGTGCGTCTTGTAA	GCCTGTATGTGTAGGAGAATGGT
GAPDH	AATGGATTTGGACGCATTGGT	TTTGCACTGGTACGTGTTGAT

Table 2. Primer sequences used in RT-qPCR. *RT-qPCR* reverse transcription quantitative polymerase chain reaction; *miR* microRNA; *RNU* spliceosomal RNAs; *TNF* tumor necrosis factor; *IL* interleukin; *TSC1* tuberous sclerosis complex 1; *ID4* inhibitor of differentiation 4; *PAX9* paired box 9; *PLEKHH1* pleckstrin homology, MyTH4 and FERM domain containing H1; *NRP2* neuropilin-2; *TMCC1* transmembrane and coiled-coil domain family 1; *RUNX1* Runt-related transcription factor 1; *CDR2* complementarity determining region 2; *B4GALT3* beta-1,4-galactosyltransferase 3; *SYNRG* synergin gamma; *HIPK2* homeodomain-interacting protein kinase 2; *SEMA7A* semaphorin 7A; *RELN* reelin; *PDK4* pyruvate dehydrogenase kinase 4; *ST6GALNAC3* ST6 N-acetylgalactosaminide alpha-2,6-sialyltransferase 3; *GAPDH* glyceraldehyde-phosphate dehydrogenase.

target for miR-27a-3p. Finally, we screened the fifteen target genes that were co-expressed in the three databases for further analysis.

Cell culture and treatment

Human embryonic kidney (HEK)-293 T cells were purchased from the Cell Bank of the Chinese Academy of Sciences (Shanghai, China) and maintained in the DMEM (Thermo Fisher) containing 10% FBS and 1% penicillin/streptomycin. All cells were incubated in a humidified incubator at 37 °C with 5% CO_2. HEK-293 T cells were transfected by miR-27a-3p inhibitor (antimiR-27a-3p; 60 nM; Sigma) or negative control miR-27a-3p (antimiR-NC; 60 nM; Sigma).

Dual-luciferase reporter assay

The cDNA sequences of TSC1 was cloned into the pGL3 luciferase reporter vector (Genecreate, Biotech Co., Ltd., Wuhan, China) to generate pGL3-wild type (WT) plasmids. Introduction of mutations into pGL3-WT yielded pGL3-mutant type (MUT) plasmids using the QuikChange II Site-Directed Mutagenesis kit (Agilent Technologies, Inc.). Subsequently, HEK-293 T were transfected with pGL3-WT and pGL3-MUT using Lipofectamine 3000 (Thermo Fisher) for 48 h. Luciferase activity was then measured with the Dual-Luciferase® Reporter Assay System Kit (Promega, Madison, WI, USA) and normalized to the activity of Renilla luciferase. The ratio of firefly to Renilla luciferase activity was calculated as the relative luciferase activity.

RNA immunoprecipitation (RIP) assay

RIP assay was employed to investigate the interaction between TSC1 and miR-27a-3p in HEK-293 T cells by a commercial RIP Kit (Geneseed Biotech Co., Ltd., Guangzhou, China). HEK-293 T cells were lysed in 400 μL complete RIP lysis buffer at 4 °C for 30 min. Following centrifugation (12,000 rpm, 10 min), the cell supernatant was harvested. The supernatant (100 μL) was designated as the Input group, while 900 μL of supernatant underwent pre-treatment with protein A + G beads at 4 °C for 10 min. Subsequently, protein A + G beads (200 μL) were combined with antibodies at 4 °C for 2 h. The antibody-bead complex was then incubated with the supernatant at 4 °C for 12 h. Following the washing steps, RNA extraction was performed, and the expression of TSC1 was quantified using qPCR.

Statistical analysis

Statistical analysis for miR-seq was performed using the hypergeometric distribution method. The SPSS 21.0 software was used to analyze data. Data are expressed as mean ± standard deviation (SD). Student's *t*-test was used for comparison between the two groups. Statistical analyses were performed using GraphPad Prism software (v8.0.1, GraphPad Software Inc., San Diego, CA, USA). Categorical variables were compared between groups using Pearson's $\chi 2$ test. $p < 0.05$ indicates that the difference is statistically significant.

Ethics approval and consent to participate

The human study was performed in line with the principles of the Declaration of Helsinki. Approval was granted by the Ethics Committee of Hainan Eye Hospital and Key Laboratory of Ophthalmology, Zhongshan Ophthalmic Center, Sun Yat-sen University. All methods were carried out in accordance with relevant guidelines and regulations. All methods are reported in accordance with ARRIVE guidelines for the reporting of animal experiments.

Results

Increased expression of miR-27a-3p in LPS-treated retina tissues

Rats were treated with LPS for 0 h, 24 h, 3d, and 7 d, and H&E staining was performed to visualize the injury of retina tissues. The results showed that after LPS treated for 24 h, intraocular neutrophils were infiltrated and the blood-eye barrier was destructed in rat retina tissues. With the extension of LPS treatment time (3 d and 7 d), the number of intraocular inflammatory cells was decreased and neutrophils were disappeared (Fig. 1A). Therefore, LPS treatment for 24 h was selected for subsequent experiments. The significantly differentially expressed miRs between the control and LPS groups were illustrated in the heatmap (Fig. 1B) and volcanic map (Fig. 1C). MiR-27a-3p was upregulated in the LPS group (Fig. 1B,C). The role of miR-27a-3p in IE has not been studied, thus we explored this in the present study. The mRNA levels of IL-1β and TNF-α in vitreous samples were increased in the LPS group compared with that in the control group (Fig. 1D,E).

Increased expression of miR-27a-3p in vitreous from patients with IE

Via RT-qPCR analysis, we observed a significant upregulation of miR-27a-3p in vitreous samples obtained from patients diagnosed with IE, in comparison to the control cohort (Fig. 2A). To further delineate the clinical relevance of this finding, we quantified miR-27a-3p expression in vitreous samples from a cohort of 31 IE patients. Based on these measurements, patients were stratified into two groups: those exhibiting miR-27a-3p expression above the calculated median were designated as the 'High' expression group, whereas individuals with expression levels at or below the median were categorized into the 'Low' expression group. Statistical evaluation revealed no significant disparity in patient age between the 'High' and 'Low' miR-27a-3p expression groups (Fig. 2B).

Clinical characteristics of the study population

As shown in Table 1, a total of 54 patients, including 31 patients with IE (male, 17; female, 14) and 23 non-infectious controls (male, 13; female, 10) were recruited in the present study. Patients with IE were caused by surgery, trauma, endogeny, and the controls were Macular hole/macular edema or rhegmatogenous retinal

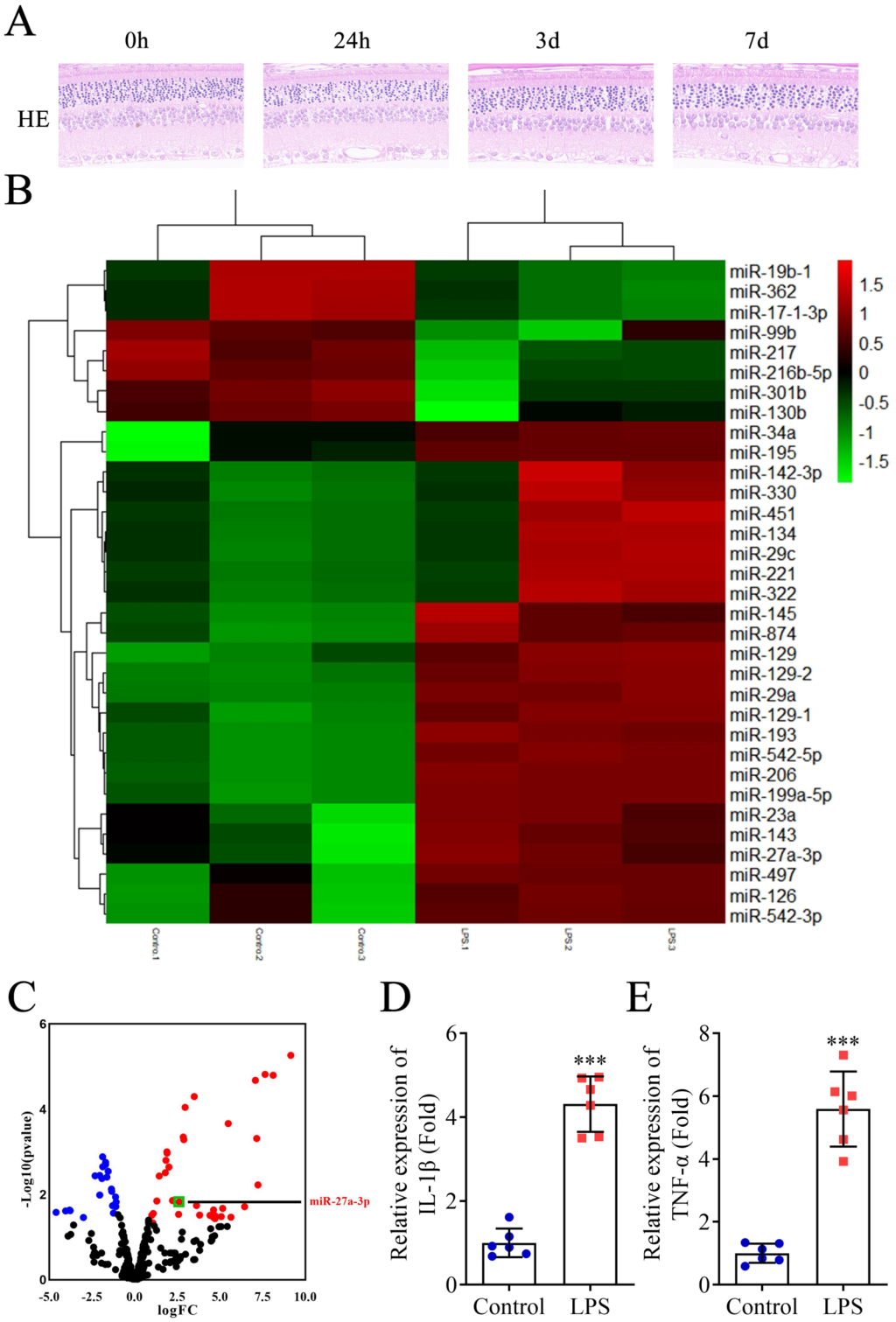

Figure 1. Increased expression of miR-27a-3p in LPS-treated retina tissues. (**A**) H&E staining of retina tissues at 0 h, 24 h, 3 d, and 7 d after LPS injection; (**B**) Differentially expressed miRs between the control and LPS groups are shown using heatmap; (**C**) Upregulated (red), downregulated (blue), and non-significant miRs (black) between the control and LPS groups using volcano plot; The mRNA levels of (**D**) IL-1β and (**E**) TNF-α in vitreous samples in the control and LPS groups were measured by RT-qPCR. ($^{***}p < 0.001$). *LPS* lipopolysaccharide; *H&E* Hematoxylin–eosin; *IE* infectious endophthalmitis; *IL-1β* interleukin-1β; *TNF-α* tumor necrosis factor receptor-α; *RT-qPCR* reverse transcription-polymerase chain reaction; *miR-27a-3p* microRNA-27a-3p.

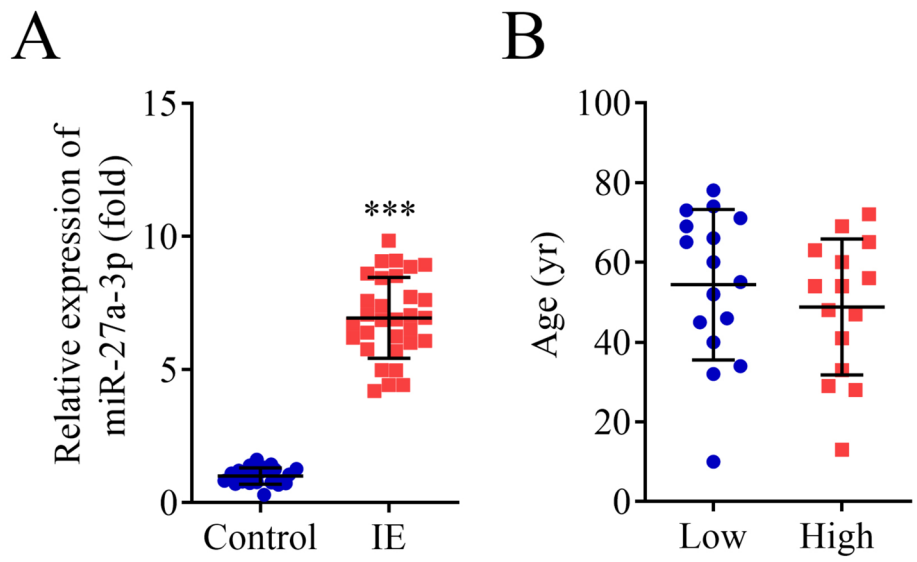

Figure 2. Increased expression of miR-27a-3p in vitreous from patients with IE. (**A**) RT-qPCR was used to detect the expression of miR-27a-3p in vitreous samples from control and IE groups; (**B**) According to the expression level of miR-27a-3p, 31 IE patients were divided into high expression (High) group and low expression (Low) group. The age between the two groups was compared by Student's *t*-test. (***$p < 0.001$). *IE* infectious endophthalmitis; *RT-qPCR* reverse transcription-quantitative polymerase chain reaction; *miR-27a-3p* microRNA-27a-3p.

detachment. There were no differences in age, sex, initial VA, final VA, inflammation/polymorphs (vitreous), surgical interventions, and pathogenic microorganisms between the control and IE groups.

Increased pro-inflammatory cytokines levels in patients with high miR-27a-3p expression

The concentration ranges of inflammatory cytokines are shown in Table 3. Compared with the 'Low' expression group, the 'High' expression group exhibited significantly elevated concentrations of IL-1α, IL-1β, IL-6, IL-8, IL-10, TNF-α, and IFN-γ (Fig. 3A–G). Notably, the GM-CSF level did not exhibit any significant differences between the two groups (Fig. 3H).

TSC1 is a target gene of miR-27a-3p

The Targetscan, starbase, and miRDB databases were used to predict the suspicious target for miR-27a-3p. Results indicated that fifteen target genes that were co-expressed in these three databases (Fig. 4A). After transfecting antimiR-27a-3p into HEK-293 T cells, the expression of miR-27a-3p was suppressed (Fig. 4B). Next, RT-qPCR was performed to detect the mRNA levels of fifteen possible target genes of miR-27a-3p. The findings suggested that after miR-27a-3p inhibition, the mRNA level of TSC1 was upregulated, while the expression of other fourteen genes showed no significant changes after miR-27a-3p inhibition (Fig. 4C). The binding site of miR-27a-3p was predicted using starbase database (Fig. 4D). Furthermore, the dual-luciferase experiment validated that transfection with antimiR-27a-3p significantly increased luciferase activity in HEK-293 T cells (Fig. 4E). Moreover, RIP results implied that miR-27a-3p interacted with the mRNA of TSC1 in HEK-293 T cells (Fig. 4F).

Markers	Concentration range (pg/mL)		*p*-value
	High (n = 15)	Low (n = 16)	
IL-1α	812.4–47,692.4	4817.6–75,139.5	0.005
IL-1β	1562.1–15,521.5	2668.6–38,463.4	0.003
IL-10	94–657.7	883.1–4666	< 0.001
IL-8	422.5–4781.3	2538–15,317.9	< 0.001
IL-6	307.1–1579.5	770.6–2550.6	< 0.001
TNF-α	84.5–365.3	283.8–4369	< 0.001
IFN-γ	15.3–302.8	21.1–1588.9	< 0.001
GM-CSF	51.5–375.8	69.2–368.5	0.227

Table 3. The concentration ranges of inflammatory cytokines in the high and low groups were detected by ELISA. *IL* interlukine; *TNF-α* tumor necrosis factor α; *IFN-γ* interferon-γ; *GM-CSF* granulocyte–macrophage colony-stimulating factor; *ELISA* enzyme-linked immunosorbent assay; *miR-27a-3p* microRNA-27a-3p.

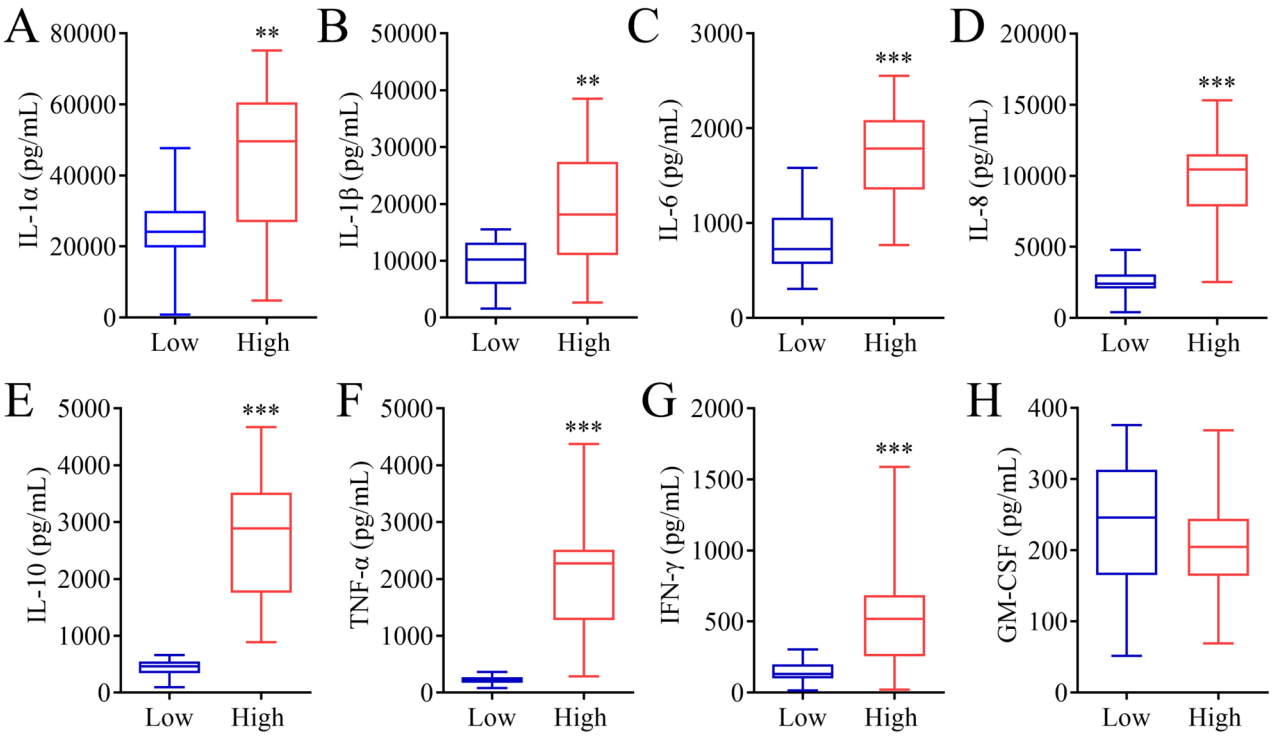

Figure 3. Increased pro-inflammatory cytokines levels in patients with high miR-27a-4p expression. The concentrations of (**A**) IL-1α, (**B**) IL-1β, (**C**) IL-6, (**D**) IL-8, (**E**) IL-10, (**F**) TNF-α, (**G**) IFN-γ, and (**H**) GM-CSF in vitreous samples were measured by ELISA. ($^{**}p < 0.01$; $^{***}p < 0.001$). *IL* interleukin; *TNF-α* tumor necrosis factor α; *IFN-γ* interferon-γ; *GM-CSF* granulocyte–macrophage colony-stimulating factor; *ELISA* enzyme-linked immunosorbent assay.

TSC1 inhibition promoted inflammation in vitreous samples

To further explore the role of miR-27a-3p and TSC1 in vivo, antagomiR-27a-3p, LV-sh-NC, and LV-sh-TSC1 were injected into rats. RT-qPCR results indicated that LPS group showed lower TSC1 expression compared with the control group (Fig. 5A). Besides, compared with the LV-sh-NC group, TSC1 inhibition showed the infiltrated intraocular neutrophils and the destructed blood-eye barrier in rat retina tissues (Fig. 5B). In addition, in contrast to the LPS group, the concentration of IL-1α, IL-1β, IL-6, IL-8, TNF-α, and IFN-γ in vitreous samples in LV-sh-NC group were decreased. Moreover, the IL-10 and GM-CSF contents were increased in LV-sh-NC group in comparison to the LPS group. Furthermore, compared with the LV-sh-NC group, TSC1 inhibition increased the concentration of IL-1α, IL-1β, IL-6, IL-8, TNF-α, and IFN-γ in vitreous samples, while the contents of IL-10 and GM-CSF showed reversed results (Fig. 5C–J).

Discussion

IE, a rare but severe form of ocular inflammation, typically arises from microbial invasion of ocular tissues. Our study utilized a rat model of IE, established through intravitreal injection of LPS, to investigate the underlying mechanisms. We observed that a 24-h LPS exposure triggered infiltration of intraocular neutrophils and disruption of the blood-eye barrier in rat retinal tissues, indicative of a robust inflammatory response. Comparative analysis of miRNA expression profiles between control and LPS-treated groups revealed a significant upregulation of miR-27a-3p in the latter. Notably, the role of miR-27a-3p in IE had not been previously explored, prompting us to delve deeper into its potential implications in this context. Elevated mRNA levels of IL-1β and TNF-α were detected in the LPS group, highlighting the induction of an inflammatory cascade in response to IE. IL-1β and TNF-α are prototypical pro-inflammatory cytokines, central to the inflammatory process. A parallel study demonstrates that endophthalmitis induced by intravitreal injection of Candida albicans results in sustained ocular inflammation and heightened levels of IL-1β, IL-6, and TNF-α[20]. Moreover, the accumulation of various pro-inflammatory factors in ocular fluids and retina tissues has been suggested as a potential diagnostic marker for diabetic retinopathy[21], underscoring the significance of inflammatory mediators in ocular pathologies.

Within the context of our human study, we observed an upregulation of miR-27a-3p in vitreous samples derived from patients suffering from IE. Strikingly, subjects exhibiting high miR-27a-3p expression also displayed elevated concentrations of IL-1α, IL-1β, IL-6, IL-8, IL-10, TNF-α, and IFN-γ within their vitreous samples. This results indicated that miR-27a-3p expression exacerbated the progression of IE via promoting inflammatory responses. Prior research corroborates our findings, demonstrating that miR-27a-3p plays a pivotal role in amplifying inflammatory reactions across diverse pathological conditions[11,22]. IE is characterized by purulent inflammation of the inner eye cavity[23], a condition where interleukins family of lymphoid factors crucial for intercellular communication and regulation of immune responses—assume a critical role[24,25]. Indeed, elevated

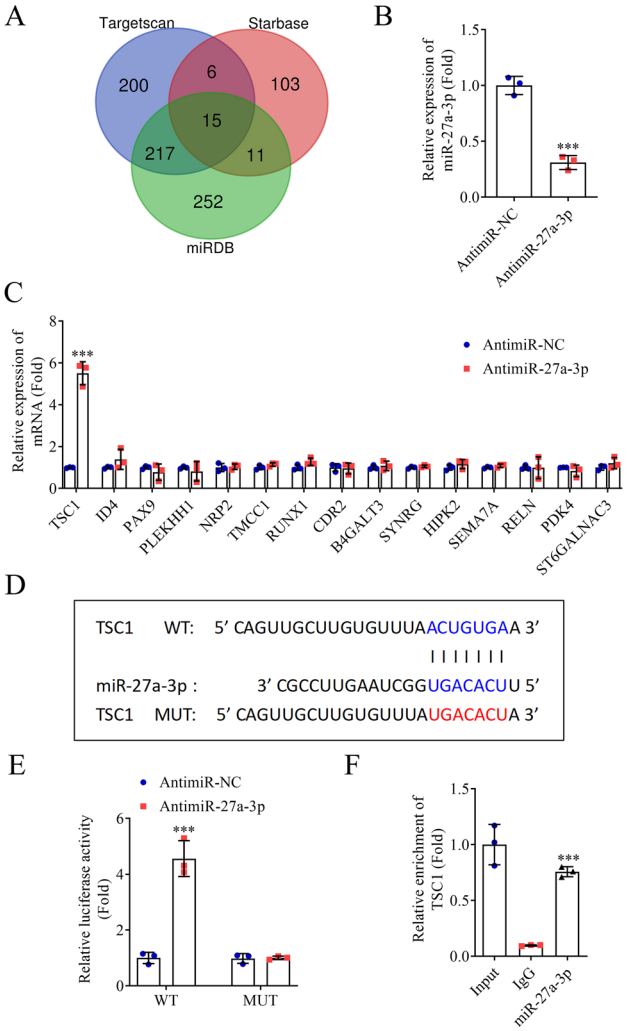

Figure 4. TSC1 is a target gene of miR-27a-3p. (**A**) The Targetscan, starbase, and miRDB databases were used to predict the suspicious target for miR-27a-3p; (**B**) RT-qPCR analysis of relative expression of miR-27a-3p; (**C**) RT-qPCR was performed to detect the mRNA levels of fifteen possible target genes of miR-27a-3p; (**D**) The binding site between miR-27a-3p and the 3'UTR of TSC1 was predicted, and the mutation site (red) was constructed; (**E**) Transfection with antimiR-27a-3p apparently increased the relative luciferase activity in HEK-293 T cells; (**F**) RIP was performed to analyze the interaction between TSC1 and miR-27a-3p in HEK-293 T cells. ($^{***}p < 0.001$). *TSC1* tuberous sclerosis complex 1; *miR* microRNA; *RT-qPCR* reverse transcription-quantitative polymerase chain reaction; *HEK* human embryonic kidney; *RIP* RNA immunoprecipitation.

levels of IL-6 and IL-10 in vitreous samples have been documented in patients with IE of varied etiologies[26]. IL-8, a potent inflammatory mediator, facilitates the recruitment of polymorphonuclear leukocytes and neutrophil infiltration in the context of endophthalmitis[27]. Similarly, heightened levels of inflammatory cytokines, including IL-1α and IL-1β, have been consistently observed in patients and experimental models of bacterial IE[28–30]. A murine study further supports this, revealing elevated levels of IL-6, IL-1β, and TNF-α in the vitreous of mice afflicted with IE [20]. In addition, miR-27a-3p has been found to be involved in the progression of a variety of diseases by regulating inflammatory responses[31,32]. Whereas, the role of miR-27a-3p in IE has not been investigated. Our study represents the pioneering exploration of miR-27a-3p's regulatory impact on IE.

TSC1 is a tumor suppressor gene that encodes the growth suppressor protein, hamartin[33]. In the present study, we found that TSC1 is a target gene of miR-27a-3p. Similarly, TSC1 is a function target of miR-27a-3p and the modulation of miR-27a-3p/TSC1 axis could be regarded as to be an effective strategy for multiple myeloma treatment[34]. Besides, TSC1 is also involved in the regulation of various diseases by serving as a target of other miRs, such as miR-301a and miR-222-3p[35,36]. We also discovered that TSC1 inhibition promoted inflammation in vitreous samples, suggesting that miR-27a-3p promoted inflammatory response in IE via targeting TSC1. The role of TSC1 in IE has not been investigated. However, stabilizing TSC1 expression has been shown to regulate a variety of inflammatory diseases, such as colitis and sterile inflammatory liver injury[37,38].

In conclusion, miR-27a-3p promoted inflammatory response in IE via targeting TSC1, suggesting that miR-27a-3p could be used as a biomarker for the diagnosis of IE. In the future, miR-27a-3p inhibitors could be developed for use in IE patients. The novelty and significance of this study is that for the first time, we have

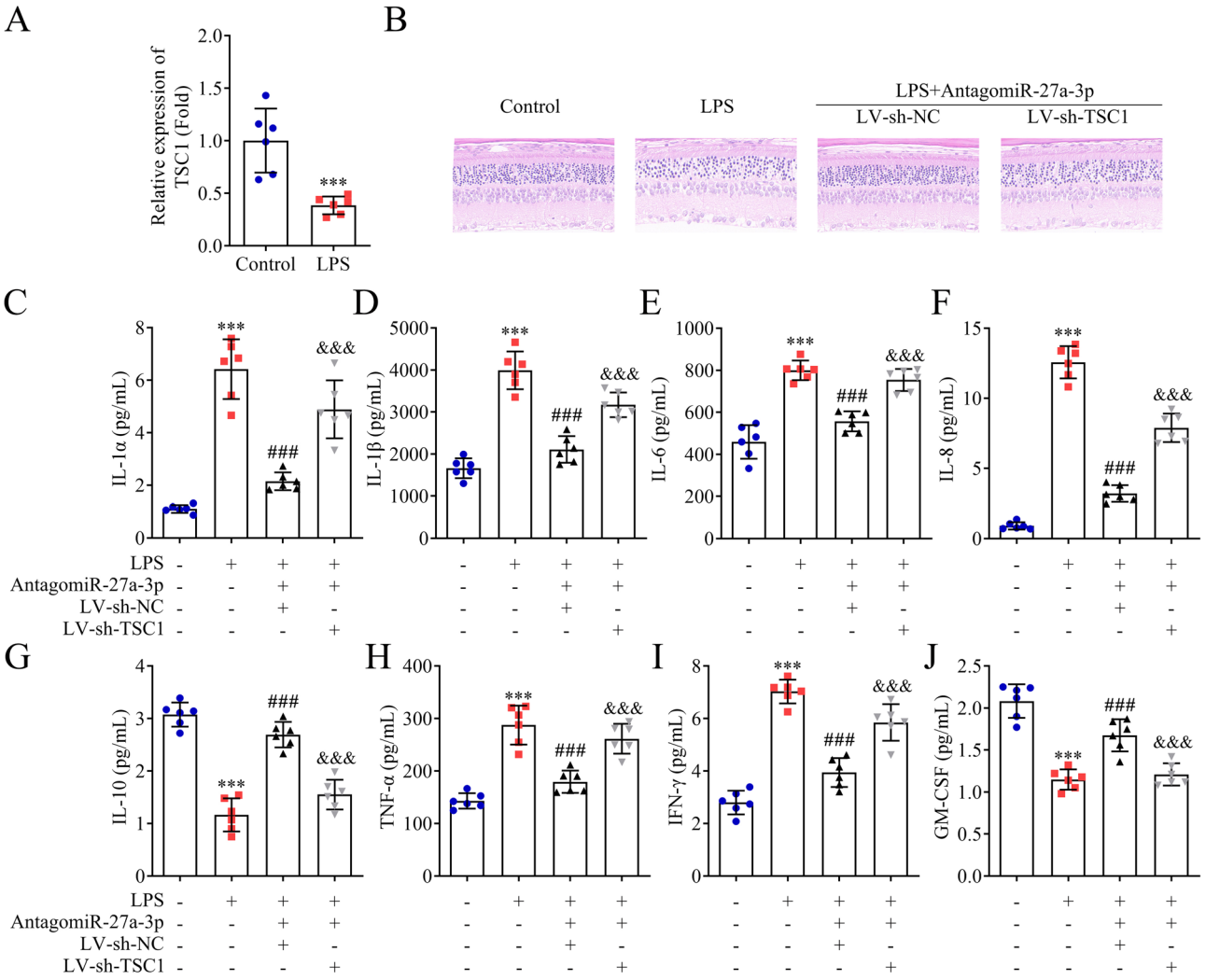

Figure 5. TSC1 inhibition promoted inflammation in vitreous samples. (**A**) RT-qPCR analysis of relative expression of TSC1; (**B**) H&E staining of retina tissues in each group; The concentrations of (**C**) IL-1α, (**D**) IL-1β, (**E**) IL-6, (**F**) IL-8, (**G**) IL-10, (**H**) TNF-α, (**I**) IFN-γ, and (**J**) GM-CSF in vitreous samples were measured by ELISA. ($^{***}p < 0.001$ vs. the control group; $^{\#\#\#}p < 0.001$ vs. the LPS group; $^{\&\&\&}p < 0.001$ vs. the LPS + AntagomiR-27a-3p + LV-sh-NC group). *TSC1* tuberous sclerosis complex 1; *RT-qPCR* reverse transcription-quantitative polymerase chain reaction; *H&E* Hematoxylin–eosin; *IL* interleukin; *TNF-α* tumor necrosis factor α; *IFN-γ* interferon-γ; *GM-CSF* granulocyte–macrophage colony-stimulating factor; *ELISA* enzyme-linked immunosorbent assay; *LPS* lipopolysaccharide; *LV* lentivirus; sh-, short hairpin.

discovered the role of miR in IE. Despite these insights, the intricate mechanisms by which miR-27a-3p influences the secretion of inflammatory cytokines remain elusive. First, our study lacked research on inflammatory signaling pathways. Besides, whether miR-27a-3p could be used as a biomarker of IE severity or prognosis remains unknown. We will further explore these limitations in our future studies.

Data availability

The datasets used and/or analyzed during the current study are available from the corresponding author on reasonable request.

Received: 6 March 2024; Accepted: 12 August 2024
Published online: 21 August 2024

References

1. Behlau, I. *et al.* Infectious endophthalmitis in boston keratoprosthesis: Incidence and prevention. *Acta Ophthalmol.* **92**(7), e546–e555. https://doi.org/10.1111/aos.12309 (2014).
2. Monteiro, J. P. *et al.* Vitreous humor in the pathologic scope: Insights from proteomic approaches. *Proteom. Clin. Appl.* **9**(1–2), 187–202. https://doi.org/10.1002/prca.201400133 (2015).
3. Ching, W. H. D. *et al.* A review of the role of intravitreal corticosteroids as an adjuvant to antibiotics in infectious endophthalmitis. *Ocul. Immunol. Inflamm.* **26**(3), 461–468. https://doi.org/10.1080/09273948.2016.1245758 (2018).

4. Brockhaus, L., Goldblum, D., Eggenschwiler, L., Zimmerli, S. & Marzolini, C. Revisiting systemic treatment of bacterial endophthalmitis: A review of intravitreal penetration of systemic antibiotics. *Clin. Microbiol. Infect.* **25**(11), 1364–1369. https://doi.org/10.1016/j.cmi.2019.01.017 (2019).
5. Soon, M. Y., Allen, P. J. & Dawkins, R. Cytokine expression in staphylococcal and streptococcal endophthalmitis. *Biomed. Hub* **7**(2), 88–98. https://doi.org/10.1159/000525330 (2022).
6. Yang, X., Tian, Y., Zheng, L., Luu, T. & Kwak-Kim, J. The update immune-regulatory role of pro- and anti-inflammatory cytokines in recurrent pregnancy losses. *Int. J. Mol. Sci.* **24**(1), 132. https://doi.org/10.3390/ijms24010132 (2022).
7. Gupta, N., Singh, P. K., Revankar, S. G., Chandrasekar, P. H. & Kumar, A. Pathobiology of *Aspergillus fumigatus* endophthalmitis in immunocompetent and immunocompromised mice. *Microorganisms* **7**(9), 297. https://doi.org/10.3390/microorganisms7090297 (2019).
8. Kinuthia, U. M., Wolf, A. & Langmann, T. Microglia and inflammatory responses in diabetic retinopathy. *Front. Immunol.* **11**, 564077. https://doi.org/10.3389/fimmu.2020.564077 (2020).
9. Hu, X. *et al.* Interplay between muller cells and microglia aggravates retinal inflammatory response in experimental glaucoma. *J. Neuroinflamm.* **18**(1), 303. https://doi.org/10.1186/s12974-021-02366-x (2021).
10. Lu, X. *et al.* Mir-27a-3p promotes non-small cell lung cancer through slc7a11-mediated-ferroptosis. *Front. Oncol.* **11**, 759346. https://doi.org/10.3389/fonc.2021.759346 (2021).
11. Zeng, Z. *et al.* Mir-27a-3p targets glp1r to regulate differentiation, autophagy, and release of inflammatory factors in pre-osteoblasts via the ampk signaling pathway. *Front. Genet.* **12**, 783352. https://doi.org/10.3389/fgene.2021.783352 (2021).
12. Li, W., Zhu, Q., Xu, X. & Hu, X. Mir-27a-3p suppresses cerebral ischemia-reperfusion injury by targeting foxo1. *Aging (Albany Ny)* **13**(8), 11727–11737. https://doi.org/10.18632/aging.202866 (2021).
13. Yao, X. *et al.* Endoplasmic reticulum stress-induced exosomal mir-27a-3p promotes immune escape in breast cancer via regulating pd-l1 expression in macrophages. *J. Cell. Mol. Med.* **24**(17), 9560–9573. https://doi.org/10.1111/jcmm.15367 (2020).
14. Xiao, M. *et al.* Mir-27a-3p and mir-30b-5p inhibited-vitamin d receptor involved in the progression of tuberculosis. *Front. Microbiol.* **13**, 1020542. https://doi.org/10.3389/fmicb.2022.1020542 (2022).
15. Hermenean, A. *et al.* Changes in retinal structure and ultrastructure in the aged mice correlate with differences in the expression of selected retinal mirnas. *Front. Pharmacol.* **11**, 593514. https://doi.org/10.3389/fphar.2020.593514 (2020).
16. Lazzara, F. *et al.* Stabilization of hif-1alpha in human retinal endothelial cells modulates expression of mirnas and proangiogenic growth factors. *Front. Pharmacol.* **11**, 1063. https://doi.org/10.3389/fphar.2020.01063 (2020).
17. Iannotta, M. *et al.* N-palmitoyl-d-glucosamine, a natural monosaccharide-based glycolipid, inhibits tlr4 and prevents lps-induced inflammation and neuropathic pain in mice. *Int. J. Mol. Sci.* **22**(3), 1491. https://doi.org/10.3390/ijms22031491 (2021).
18. Lu, J., Zhou, N., Yang, P., Deng, L. & Liu, G. Microrna-27a-3p downregulation inhibits inflammatory response and hippocampal neuronal cell apoptosis by upregulating mitogen-activated protein kinase 4 (map2k4) expression in epilepsy: In vivo and in vitro studies. *Med. Sci. Monit.* **25**, 8499–8508. https://doi.org/10.12659/MSM.916458 (2019).
19. Kaneko, H. *et al.* Better visual outcome by intraocular lens ejection in geriatric patients with ruptured ocular injuries. *Plos One* **12**(1), e0170094. https://doi.org/10.1371/journal.pone.0170094 (2017).
20. Rottmann, B. G. *et al.* Evaluation of susceptibility and innate immune response in c57bl/6 and balb/c mice during *Candida albicans* endophthalmitis. *Invest. Ophthalmol. Vis. Sci.* **61**(11), 31. https://doi.org/10.1167/iovs.61.11.31 (2020).
21. Shahulhameed, S. *et al.* A systematic investigation on complement pathway activation in diabetic retinopathy. *Front. Immunol.* **11**, 154. https://doi.org/10.3389/fimmu.2020.00154 (2020).
22. Liao, Y. *et al.* Microrna-27a-3p directly targets fosb to regulate cell proliferation, apoptosis, and inflammation responses in immunoglobulin a nephropathy. *Biochem. Biophys. Res. Commun.* **529**(4), 1124–1130. https://doi.org/10.1016/j.bbrc.2020.06.115 (2020).
23. Haseeb, A. A., Elhusseiny, A. M., Siddiqui, M. Z., Ahmad, K. T. & Sallam, A. B. Fungal endophthalmitis: A comprehensive review. *J. Fungi (Basel)* **7**(11), 996. https://doi.org/10.3390/jof7110996 (2021).
24. Zhu, H. *et al.* Interleukins and ischemic stroke. *Front. Immunol.* **13**, 828447. https://doi.org/10.3389/fimmu.2022.828447 (2022).
25. Wu, Y. *et al.* Interleukin 22 in liver injury, inflammation and cancer. *Int. J. Biol. Sci.* **16**(13), 2405–2413. https://doi.org/10.7150/ijbs.38925 (2020).
26. Kuo, D. E. *et al.* Gradient boosted decision tree classification of endophthalmitis versus uveitis and lymphoma from aqueous and vitreous il-6 and il-10 levels. *J. Ocul. Pharmacol. Ther.* **33**(4), 319–324. https://doi.org/10.1089/jop.2016.0132 (2017).
27. Naik, P. *et al.* Multidrug-resistant pseudomonas aeruginosa triggers differential inflammatory response in patients with endophthalmitis. *Transl. Vis. Sci. Technol.* **10**(9), 26. https://doi.org/10.1167/tvst.10.9.26 (2021).
28. Talreja, D., Singh, P. K. & Kumar, A. In vivo role of tlr2 and myd88 signaling in eliciting innate immune responses in staphylococcal endophthalmitis. *Invest. Ophthalmol. Vis. Sci.* **56**(3), 1719–1732. https://doi.org/10.1167/iovs.14-16087 (2015).
29. Shamsuddin, N. & Kumar, A. Tlr2 mediates the innate response of retinal muller glia to *Staphylococcus aureus*. *J. Immunol.* **186**(12), 7089–7097. https://doi.org/10.4049/jimmunol.1100565 (2011).
30. Kumar, A., Singh, P. K., Ahmed, Z., Singh, S. & Kumar, A. Essential role of nlrp3 inflammasome in mediating il-1beta production and the pathobiology of *Staphylococcus aureus* endophthalmitis. *Infect. Immun.* **90**(5), e0010322. https://doi.org/10.1128/iai.00103-22 (2022).
31. Fan, H. & Zhang, W. Overexpression of linc 4930556m19rik suppresses high glucose-triggered podocyte apoptosis, fibrosis and inflammation via the mir-27a-3p/metalloproteinase 3 (timp3) axis in diabetic nephropathy. *Med. Sci. Monit.* **26**, e925361. https://doi.org/10.12659/MSM.925361 (2020).
32. Shang, J. *et al.* Mir-27a-3p overexpression mitigates inflammation and apoptosis of lipopolysaccharides-induced alveolar epithelial cells by targeting foxo3 and suppressing the activation of napdh/ros. *Biochem. Biophys. Res. Commun.* **533**(4), 723–731. https://doi.org/10.1016/j.bbrc.2020.07.126 (2020).
33. Shimobayashi, M. & Hall, M. N. Making new contacts: The mtor network in metabolism and signalling crosstalk. *Nat. Rev. Mol. Cell Biol.* **15**(3), 155–162. https://doi.org/10.1038/nrm3757 (2014).
34. Wang, Y. *et al.* Long non-coding rna oip5-as1 suppresses multiple myeloma progression by sponging mir-27a-3p to activate tsc1 expression. *Cancer Cell Int.* **20**, 155. https://doi.org/10.1186/s12935-020-01234-7 (2020).
35. Wang, J. *et al.* Mir-301a suppression within fibroblasts limits the progression of fibrosis through the tsc1/mtor pathway. *Mol. Ther. Nucleic Acids* **21**, 217–228. https://doi.org/10.1016/j.omtn.2020.05.027 (2020).
36. Guo, Y. *et al.* Mir-222-3p-containing macrophage-derived extracellular vesicles confer gemcitabine resistance via tsc1-mediated mtor/akt/pi3k pathway in pancreatic cancer. *Cell Biol. Toxicol.* **39**(4), 1203–1214. https://doi.org/10.1007/s10565-022-09736-y (2023).
37. Wang, X. *et al.* The m6a reader igf2bp2 regulates macrophage phenotypic activation and inflammatory diseases by stabilizing tsc1 and ppargamma. *Adv. Sci. (Weinh)* **8**(13), 2100209. https://doi.org/10.1002/advs.202100209 (2021).
38. Ni, M. *et al.* Loss of macrophage tsc1 exacerbates sterile inflammatory liver injury through inhibiting the akt/mst1/nrf2 signaling pathway. *Cell Death Dis.* **15**(2), 146. https://doi.org/10.1038/s41419-024-06538-4 (2024).

Author contributions

All authors contributed to the study conception and design. Material preparation, data collection and analysis were performed by S.L. and H.H. The first draft of the manuscript was written by Y.C. and all authors commented on previous versions of the manuscript. All authors read and approved the final manuscript.

Funding

The work was supported by Hainan Provincial Natural Science Foundation Youth Foundation Project under grant number 822QN481; Hainan Province Clinical Medical Center.

Competing interests

The authors declare no competing interests.

Additional information

Correspondence and requests for materials should be addressed to Y.C.

Reprints and permissions information is available at www.nature.com/reprints.

Publisher's note Springer Nature remains neutral with regard to jurisdictional claims in published maps and institutional affiliations.